



# Matrix isolation infrared spectroscopic study of 4-Pyridinecarboxaldehyde and of its UV-induced photochemistry



Liesel Cluyts<sup>a,b</sup>, Archana Sharma<sup>b</sup>, Nihal Kuş<sup>b,c</sup>, Kristien Schoone<sup>d</sup>, Rui Fausto<sup>b,\*</sup>

<sup>a</sup> Department of Chemical Engineering, Catholic University Leuven, Celestijnenlaan 200F, box 2424, B-3001 Heverlee, Belgium

<sup>b</sup> CQC, Department of Chemistry, University of Coimbra, P-3004-535 Coimbra, Portugal

<sup>c</sup> Department of Physics, Anadolu University, TR-26470 Eskişehir, Turkey

<sup>d</sup> Thomas More University, Kleinhoefstraat 4, B-2440 Geel, Belgium

## ARTICLE INFO

### Article history:

Received 6 June 2016

Received in revised form 25 July 2016

Accepted 2 August 2016

Available online 03 August 2016

### Keywords:

4-Pyridinecarboxaldehyde

Matrix isolation infrared spectroscopy

Narrowband UV-induced photochemistry

Quantum chemical calculations

## ABSTRACT

The structure, infrared spectrum, barrier to internal rotation, and photochemistry of 4-pyridinecarboxaldehyde (4PCA) were studied by low-temperature (10 K) matrix isolation infrared spectroscopy and quantum chemical calculations undertaken at both Moller-Plesset to second order (MP2) and density functional theory (DFT/B3LYP) levels of approximation. The molecule has a planar structure ( $C_s$  point group), with MP2/6-311++G(d,p) predicted internal rotation barrier of  $26.6 \text{ kJ mol}^{-1}$ , which is slightly smaller than that of benzaldehyde ( $\sim 30 \text{ kJ mol}^{-1}$ ), thus indicating a less important electron charge delocalization from the aromatic ring to the aldehyde moiety in 4PCA than in benzaldehyde. A complete assignment of the infrared spectrum of 4PCA isolated in an argon matrix has been done for the whole  $4000\text{--}400 \text{ cm}^{-1}$  spectral range, improving over previously reported data. Both the geometric parameters and vibrational frequencies of the aldehyde group reveal the relevance in this molecule of the electronic charge back-donation effect from the oxygen *trans* lone electron pair to the aldehyde C—H anti-bonding orbital. Upon in situ UV irradiation of the matrix-isolated compound, prompt decarbonylation was observed, leading to formation of pyridine.

© 2016 Elsevier B.V. All rights reserved.

## 1. Introduction

Substituted pyridines have attracted much attention due to their multiple applications. 4-Pyridinecarboxaldehyde (4PCA; Fig. 1) was shown to be an efficient building block for synthesis of Schiff bases using a Korich-type reaction [1], an intermolecular reductive synthetic procedure based on the condensation of nitro-substituted arenes and aromatic aldehydes in the presence of iron powder and dilute acid [2]. Metal complexes of several of these Schiff bases were shown to exhibit good activity against different types of bacteria (e.g., *Staphylococcus aureus*, *E. coli*, *Klebsiella*, *Pneumonia*) and fungi (*Candida albicans*, *Aspergillus niger* and *Penicillium sp*) [1,3], and also moderate nuclease activity [3]. 4PCA and some of its derivatives have also been reported as useful transamination reagents to introduce ketone or aldehyde groups onto the N-termini of antibodies [4,5] for subsequent site-specifically conjugate aminoxy-functionalized molecules (including fluorescent dyes, polyethylene glycol, or porphyrins) to these entities [5–7].

To the best of our knowledge, there are no experimental data on the structure of 4PCA molecule. However, its geometry and infrared (IR) spectrum have been investigated using both Density Functional Theory

(DFT) and Hartree-Fock (HF) theoretical approaches [8,9], the molecule being predicted to be planar at both levels of approximation. The IR spectrum of 4PCA isolated in an argon matrix at 15 K, within the range  $1900\text{--}600 \text{ cm}^{-1}$ , has been obtained by Ohno and coworkers [8], and IR and Raman spectra of the liquid compound, at room temperature, have been reported earlier by Green and Harrison [10]. Ohno and coworkers [8] described also the ultraviolet-visible (UV-Vis) spectrum of 4PCA in hexane solution at room temperature. The observed intense UV absorption ( $\epsilon = 2800 \text{ L mol}^{-1} \text{ cm}^{-1}$ ) with maximum at 283.3 nm was assigned to the  $\pi, \pi^* S_2 \leftarrow S_0$  transition, while the low-intensity bands due to the  $n, \pi^*$  transitions to  $S_1$  ( $\epsilon = 7.1 \text{ L mol}^{-1} \text{ cm}^{-1}$ ) and  $T_1$  (spin-forbidden;  $\epsilon = 0.1 \text{ L mol}^{-1} \text{ cm}^{-1}$ ) were observed at 381.7 and 411.4 nm, respectively [8].

In the present study, (i) the equilibrium geometry of 4PCA and the barrier of internal rotation of the aldehyde group were obtained at a higher-level of theory than previously reported (Moller-Plesset to second order with a triple- $\zeta$  basis set, completed with polarization functions in both heavy atoms and hydrogens as well as with diffuse functions: MP2/6-311++G(d,p)), (ii) the infrared spectrum of the compound isolated in an argon matrix was studied in an extended frequency range ( $4000\text{--}400 \text{ cm}^{-1}$ ) and fully assigned based on normal coordinates' calculations, and (iii) the UV-induced photochemistry exhibited by the matrix-isolated compound was investigated. The

\* Corresponding author.

E-mail address: [rfausto@ci.uc.pt](mailto:rfausto@ci.uc.pt) (R. Fausto).

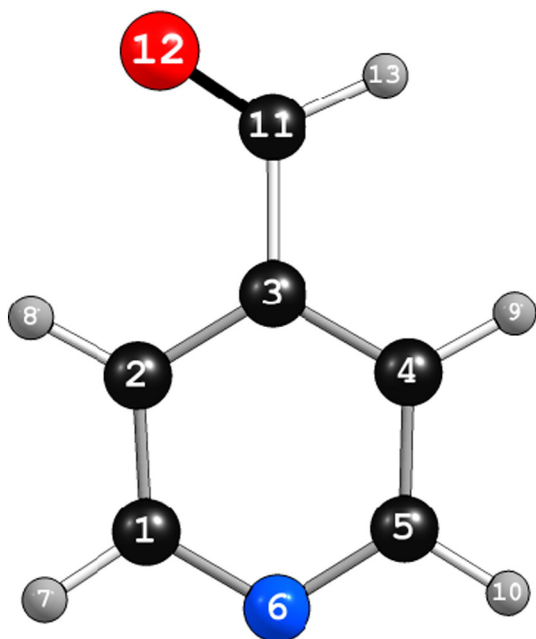


Fig. 1. 4PCA minimum energy structure with atom numbering used in this study.

present investigation thus expands the results obtained in previous studies on the structure and spectroscopy of the compound [8–10] and provides new data on its photochemistry.

## 2. Experimental and computational methods

### 2.1. Experimental details

4PCA was provided by Koch-Light Laboratories, Ltd. (purity >99%) and was further purified by the standard freeze-pump-thaw technique before experiments to remove traces of volatile impurities. Vapors of the compound at room temperature were co-deposited together with a large excess of argon (N60, supplied by Air Liquide) onto the CsI optical substrate of the cryostat kept at a temperature of 10 K. The gaseous argon was introduced in the cryostat from a separate line. The temperature of the cold substrate was measured by a silicon diode sensor connected to a digital controller (Scientific Instruments, Model 9650-1) with accuracy of  $\pm 0.1$  degree. The low temperature equipment was based on a closed-cycle helium refrigerator (APD Cryogenics) with a DE-202A expander.

Infrared spectra were registered with  $0.5 \text{ cm}^{-1}$  resolution, in the range  $4000\text{--}400 \text{ cm}^{-1}$ , using a Thermo Nicolet Nexus 670 FT-IR spectrometer, equipped with a deuterated triglycine sulphate (DTGS) detector and a KBr beamsplitter.

UV irradiations of the matrix-isolated 4PCA were performed using the narrowband ( $0.2 \text{ cm}^{-1}$  spectral width) light provided by a Spectra Physics Quanta-Ray MOPO-SL optical parametric oscillator pumped with a pulsed Spectra Physics Quanta-Ray PRO-230-10 Nd:YAG laser (repetition rate, pulse energy and duration were 10 Hz,  $\sim 5 \text{ mW}$  and 10 ns, respectively).

### 2.2. Computational details

Calculation of structures and IR spectra were performed using the Gaussian 03 program package [11]. Geometries were obtained at both the DFT and MP2 levels of theory, with the 6-311++G(d,p) basis set [12,13]. In the DFT calculations, the B3LYP hybrid functional [14–16] was used. The IR spectra were obtained at the DFT(B3LYP)/6-311++G(d,p) level, the calculated wavenumbers being subsequently

scaled down by the factor 0.978 to account for the approximations inherent to the used theoretical model and anharmonicity.

Normal coordinate analysis was performed in the internal coordinates space, as described by Schachtshneider and Mortimer [17], using the structural data and Cartesian force constants resulting from the B3LYP/6-311++G(d,p) calculations. The Cartesian force constants were converted to the space of symmetry coordinates shown in Table 1 in order to allow for the calculation of the normal modes of vibration and potential energy distributions (PEDs). These calculations were performed using a locally modified version of the program BALGA [18]. For the purpose of modeling IR spectra, the calculated wavenumbers, together with the calculated IR intensities, served to simulate the spectra shown in the figures by convoluting each peak with a Lorentzian function with a full-width-at-half-maximum (FWHM) of  $2 \text{ cm}^{-1}$ .

Table 1  
Definition of symmetry coordinates used in the normal coordinate analysis of 4PCA.<sup>a</sup>

Coordinate	Definition <sup>b</sup>	Approximate description
A'		
S <sub>1</sub>	$\nu\text{C3C11}$	$\nu\text{CC}$
S <sub>2</sub>	$\nu\text{C11O12}$	$\nu\text{C} = \text{O}$
S <sub>3</sub>	$\nu\text{C11H13}$	$\nu\text{CH}$
S <sub>4</sub>	$\nu\text{C2H8}$	$\nu\text{CH } r_1$
S <sub>5</sub>	$\nu\text{C1H7}$	$\nu\text{CH } r_2$
S <sub>6</sub>	$\nu\text{C4C9} + \nu\text{C5H10}$	$\nu\text{CH } r_3$
S <sub>7</sub>	$\nu\text{C4C9} - \nu\text{C5H10}$	$\nu\text{CH } r_4$
S <sub>8</sub>	$2\nu\text{C1C2} + 2\nu\text{C4C5} - \nu\text{C1N6} - \nu\text{N6C5} - \nu\text{C2C3} - \nu\text{C3C4}$	$\nu\tau_1$
S <sub>9</sub>	$\nu\text{C1C2} + \nu\text{C4C5} + \nu\text{C1N6} + \nu\text{N6C5} + \nu\text{C2C3} + \nu\text{C3C4}$	$\nu\tau_2$
S <sub>10</sub>	$\nu\text{C1C2} - \nu\text{C4C5}$	$\nu\tau_3$
S <sub>11</sub>	$\nu\text{C1N6} - \nu\text{N6C5} - \nu\text{C2C3} + \nu\text{C3C4}$	$\nu\tau_4$
S <sub>12</sub>	$\nu\text{C1N6} + \nu\text{N6C5} - \nu\text{C2C3} - \nu\text{C3C4}$	$\nu\tau_5$
S <sub>13</sub>	$\nu\text{C1N6} - \nu\text{N6C5} + \nu\text{C2C3} - \nu\text{C3C4}$	$\nu\tau_6$
S <sub>14</sub>	$\delta\text{O12H13C11} - \delta\text{C3H13C11}$	$\delta\text{CH}$
S <sub>15</sub>	$2\delta\text{O12C3C11} - \delta\text{O12H13C11} - \delta\text{C3H13C11}$	$\delta\text{CCO}$
S <sub>16</sub>	$\delta\text{C2C11C3} - \delta\text{C4C11C3}$	$\delta\text{CCC}$
S <sub>17</sub>	$\delta\text{C2N6C1} - \delta\text{C1C5N6} + \delta\text{N6C4C5} - \delta\text{C5C3C4} + \delta\text{C4C2C3} - \delta\text{C3C1C2}$	$\delta\tau_1$
S <sub>18</sub>	$\delta\text{C2N6C1} - 2\delta\text{C1C5N6} + \delta\text{N6C4C5} + \delta\text{C5C3C4} - 2\delta\text{C4C2C3} + \delta\text{C3C1C2}$	$\delta\tau_2$
S <sub>19</sub>	$\delta\text{C2N6C1} - \delta\text{N6C4C5} + \delta\text{C5C3C4} - \delta\text{C3C1C2}$	$\delta\tau_3$
S <sub>20</sub>	$\delta\text{C3H8C2} - \delta\text{C1H8C2} + \delta\text{C2H7C1} - \delta\text{C6H7C1} + \delta\text{C4H10C5} - \delta\text{C6H10C5} + \delta\text{C3H9C4} - \delta\text{C5H9C4}$	$\delta\text{CH } r_1$
S <sub>21</sub>	$\delta\text{C3H8C2} - \delta\text{C1H8C2} - \delta\text{C2H7C1} + \delta\text{C6H7C1} + \delta\text{C4H10C5} - \delta\text{C6H10C5} - \delta\text{C3H9C4} + \delta\text{C5H9C4}$	$\delta\text{CH } r_2$
S <sub>22</sub>	$\delta\text{C3H8C2} - \delta\text{C1H8C2} + \delta\text{C2H7C1} - \delta\text{C6H7C1} - \delta\text{C4H10C5} + \delta\text{C6H10C5} - \delta\text{C3H9C4} + \delta\text{C5H9C4}$	$\delta\text{CH } r_3$
S <sub>23</sub>	$\delta\text{C3H8C2} - \delta\text{C1H8C2} - \delta\text{C2H7C1} + \delta\text{C6H7C1} - \delta\text{C4H10C5} + \delta\text{C6H10C5} + \delta\text{C3H9C4} - \delta\text{C5H9C4}$	$\delta\text{CH } r_4$
A''		
S <sub>24</sub>	$\gamma\text{H13}-(\text{C11O12C3})$	$\gamma\text{CH}$
S <sub>25</sub>	$\gamma\text{C11}-(\text{C3C4C2})$	$\gamma\text{CC}$
S <sub>26</sub>	$\gamma\text{H8}-(\text{C2C3C1}) + \gamma\text{H7}-(\text{C1C2N6}) + \gamma\text{H10}-(\text{C5C4N6}) + \gamma\text{H9}-(\text{C4C3C5})$	$\gamma\text{CH } r_1$
S <sub>27</sub>	$\gamma\text{H8}-(\text{C2C3C1}) + \gamma\text{H7}-(\text{C1C2N6}) - \gamma\text{H10}-(\text{C5C4N6}) - \gamma\text{H9}-(\text{C4C3C5})$	$\gamma\text{CH } r_2$
S <sub>28</sub>	$\gamma\text{H8}-(\text{C2C3C1}) - \gamma\text{H7}-(\text{C1C2N6}) + \gamma\text{H10}-(\text{C5C4N6}) - \gamma\text{H9}-(\text{C4C3C5})$	$\gamma\text{CH } r_3$
S <sub>29</sub>	$\gamma\text{H8}-(\text{C2C3C1}) - \gamma\text{H7}-(\text{C1C2N6}) - \gamma\text{H10}-(\text{C5C4N6}) + \gamma\text{H9}-(\text{C4C3C5})$	$\gamma\text{CH } r_4$
S <sub>30</sub>	$\tau\text{C2C3} - \tau\text{C1C2} + \tau\text{N6C1} - \tau\text{C5N6} + \tau\text{C4C5} - \tau\text{C3C4}$	$\tau\tau_1$
S <sub>31</sub>	$\tau\text{C2C3} - \tau\text{N6C1} + \tau\text{C5N6} - \tau\text{C3C4}$	$\tau\tau_2$
S <sub>32</sub>	$\tau\text{C2C3} - 2\tau\text{C1C2} + \tau\text{N6C1} + \tau\text{C5N6} - 2\tau\text{C4C5} + \tau\text{C3C4}$	$\tau\tau_3$
S <sub>33</sub>	$\tau\text{C3C11}$	$\tau\text{CC}$

<sup>a</sup> For atom numbering, see Fig. 1.  $\nu$ , stretching;  $\delta$ , in-plane bending;  $\gamma$ , out-of-plane rocking;  $\tau$ , torsion;  $r$ , ring.

<sup>b</sup> Normalization factors not given; angles are defined with the apex atom at the end.

Download English Version:

<https://daneshyari.com/en/article/1229984>

Download Persian Version:

<https://daneshyari.com/article/1229984>

[Daneshyari.com](https://daneshyari.com)